A rhodamine-quinoline based chemodosimeter capable of recognising endogenous OCl^- in human blood cell

Shyamaprosad Goswami*[a], Sangita Das [a], Krishnendu Aich [a], Prasanta Kumar Nandi [a], Kakali Ghoshal[b], Ching Kheng Quah [c], Maitree Bhattacharyya [b], Hoong-Kun Fun[c,d], Hatem A. Abdel-Aziz [d,e]

[a]*Department of Chemistry, Bengal Engineering and Science University, Shibpur, Howrah, INDIA, 711 103, Tel. +91-33-2668 4561-3 ext. 498; Fax. +91-33-2668 2916.*

E-mail spgoswamical@yahoo.com

[b] *Department of Biochemistry, University of Calcutta, Kolkata – 700019, INDIA.*
E-mail: bmaitree@gmail.com
[c] *X–ray Crystallography Unit, School of Physics, Universiti Sains Malaysia, 11800 USM, Penang, Malaysia.*
[d] *Department of Pharmaceutical Chemistry, College of Pharmacy, King Saud University, Riyadh 11451, Saudi Arabia;*

E-mail: hfun.c@ksu.edu.sa

Tel Office : (+966) 146-77335 Fax : (+966)146-76220

[e] *Department of Applied Organic Chemistry, National Research Center, Dokki, Cairo 12622, Egypt.*

CONTENTS

1. **Time dependent fluorescence change of RHQ upon addition of OCl^- and reaction kinetics**

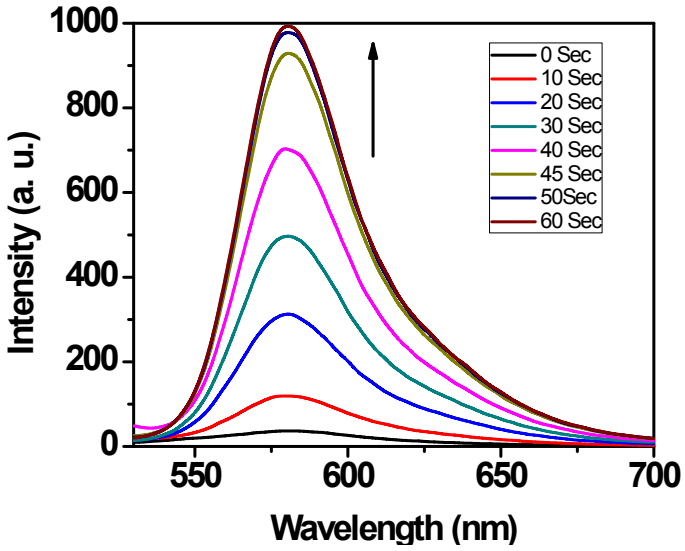

Figure S1: Change of emission spectra of RHQ (10 μM) after addition of OCl^- (2 equivalents) with time interval.

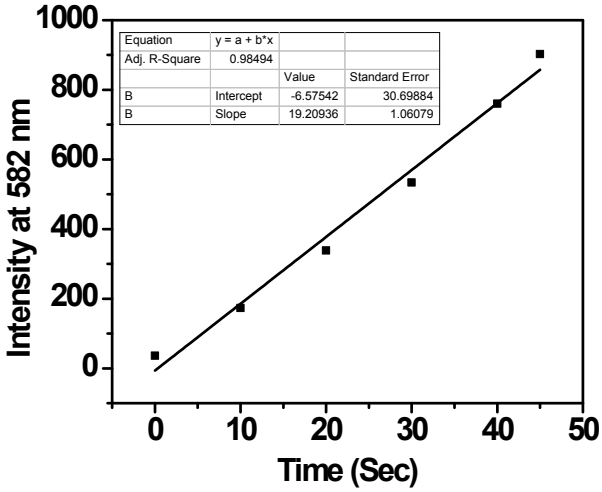

Figure S2: Time (Sec) vs. emission (I_{582}) plot

2. Determination of detection limit:

The detection limit (DL) of **RHQ** for OCl^- was determined from the following equation:

DL = K* Sb1/S

Where K = 2 or 3 (we take 3 in this case); Sb1 is the standard deviation of the blank solution; S is the slope of the calibration curve.

By fluorescence method:

From the graph, we get slope = 5.59×10^7, and Sb_1 value is 0.103634

Thus using the formula we get the Detection Limit = 5.5 x 10^{-8} M i.e. RHQ can detect OCl^- in this minimum concentration through fluorescence method.

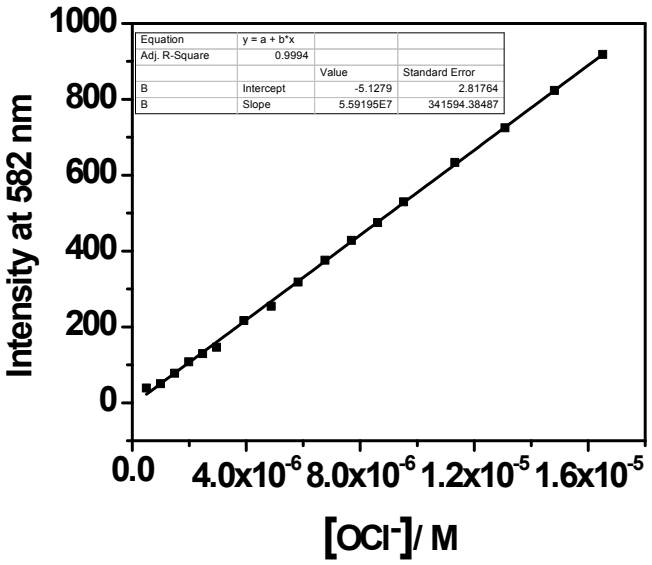

Figure S3.The linear response curve of emission intensity at 582 nm of RHQ depending on OCl^- concentration

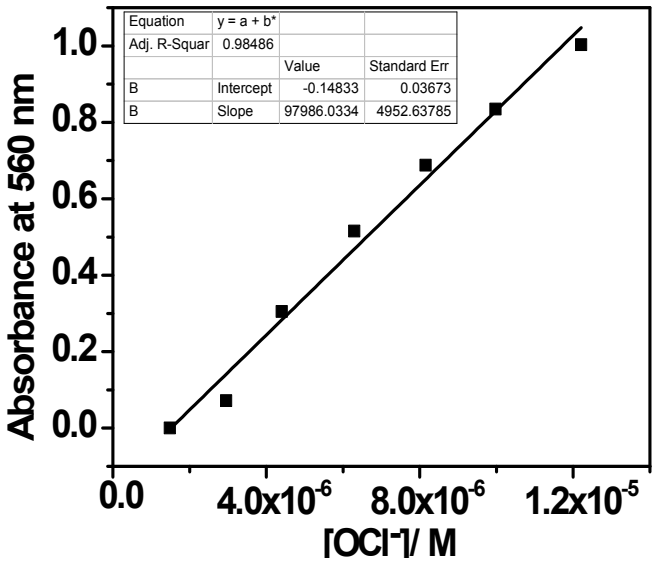

Figure S4. The linear response curve of absorbance intensity at 560 nm of RHQ depending on OCl^- concentration

3. ^{1}H NMR spectra of the receptor:

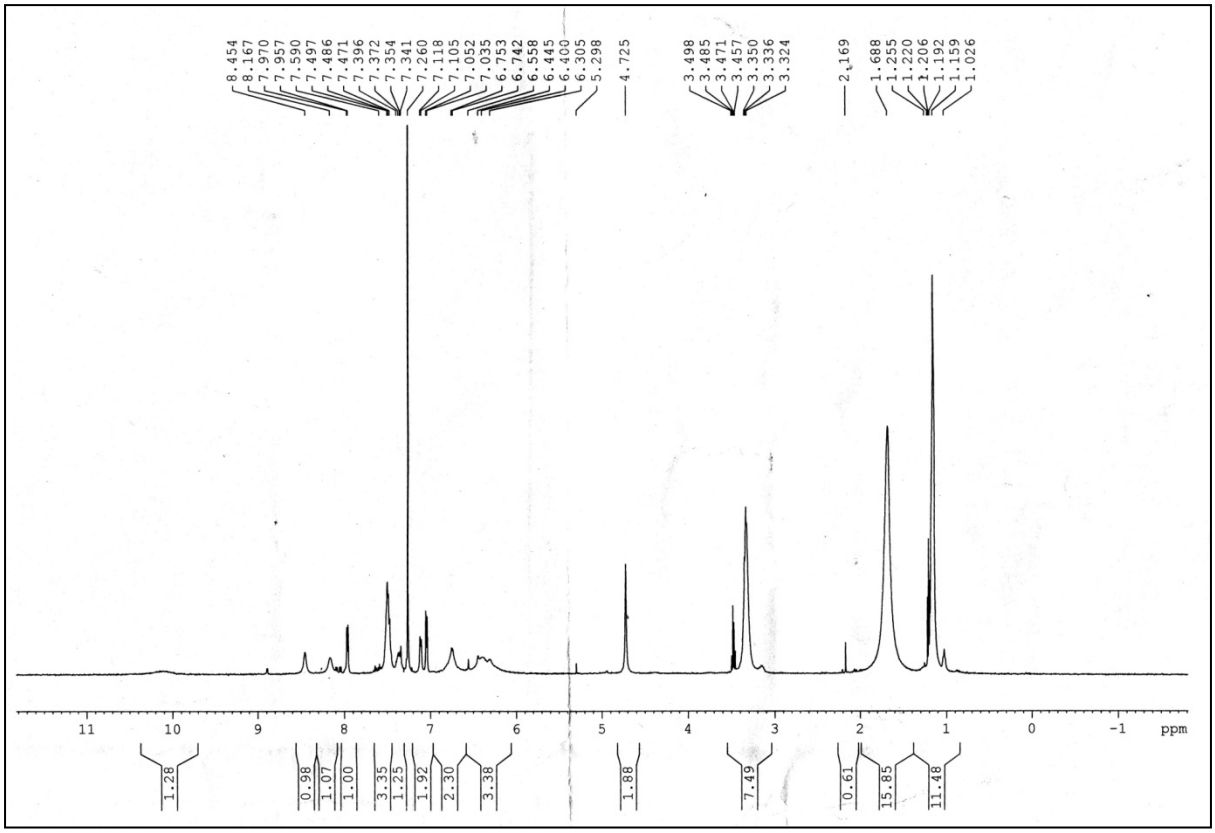

Figure S5: ^{1}H NMR (500 MHz) spectra of the receptor in $CDCl_3$

4. ESI MS spectra of the receptor:

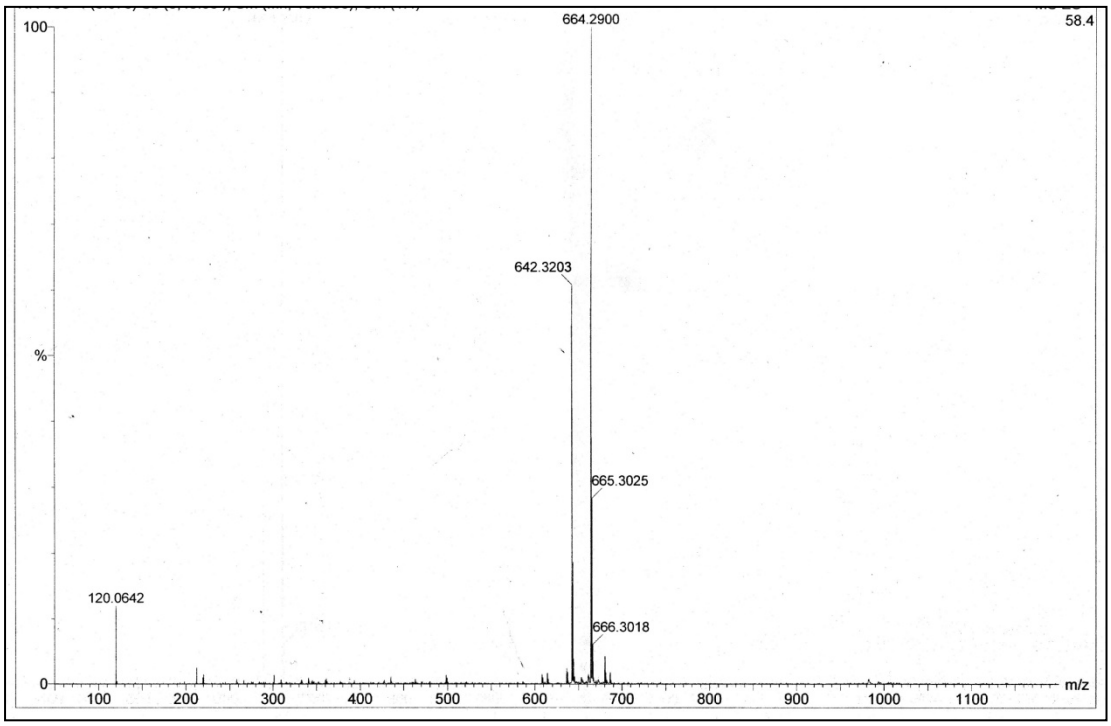

Figure S6: HRMS spectra of the receptor.

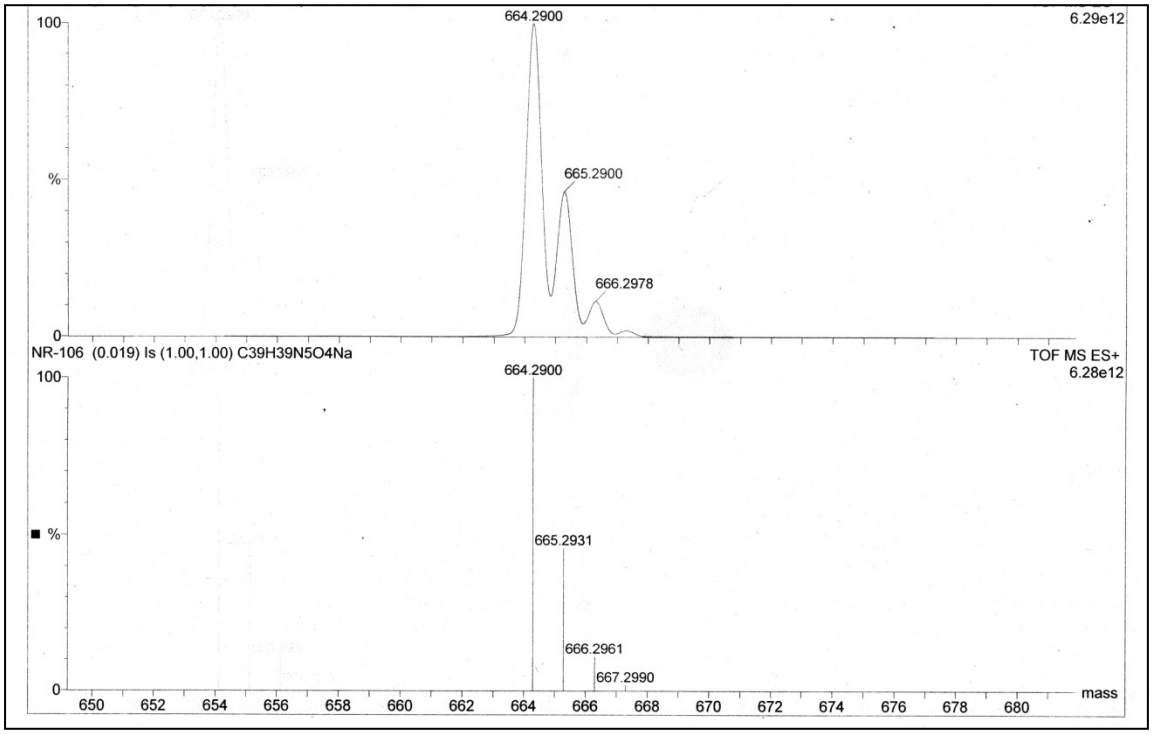

Figure S6a: HRMS (Expansion)spectra of the receptor

5. ^{13}C NMR spectra of the receptor:

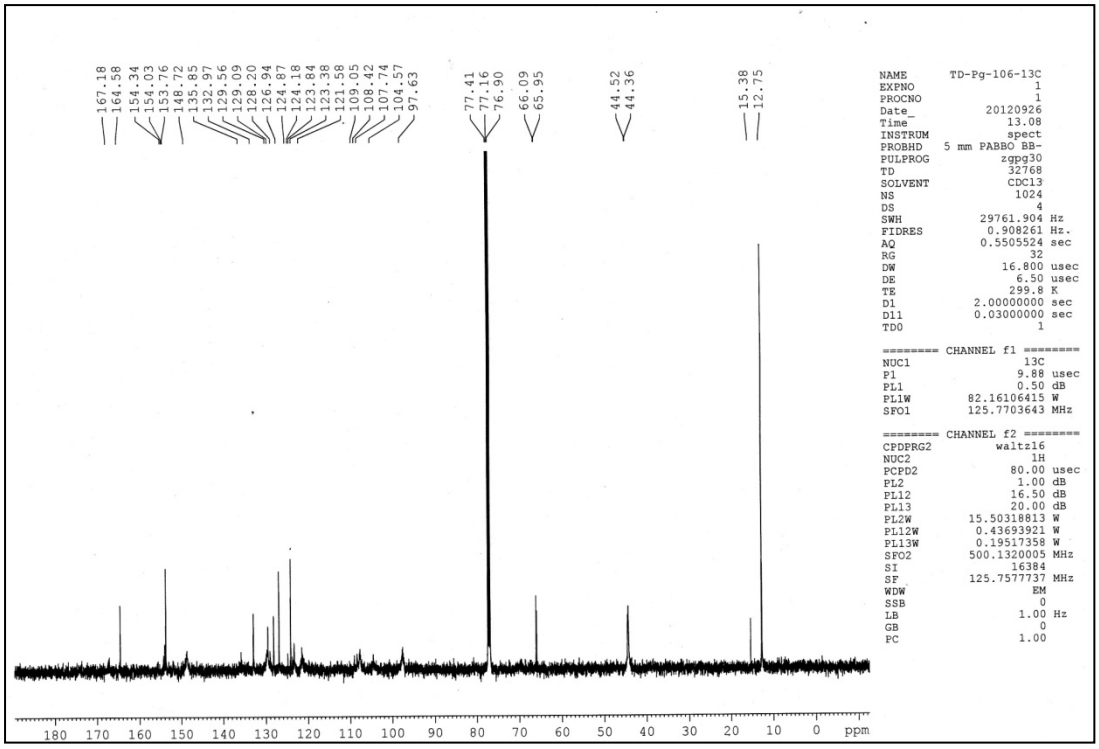

Figure S7: ^{13}C NMR (125 MHz) spectra of the receptor in $CDCl_3$.

6. HRMS of the receptor after reaction with OCl^-:

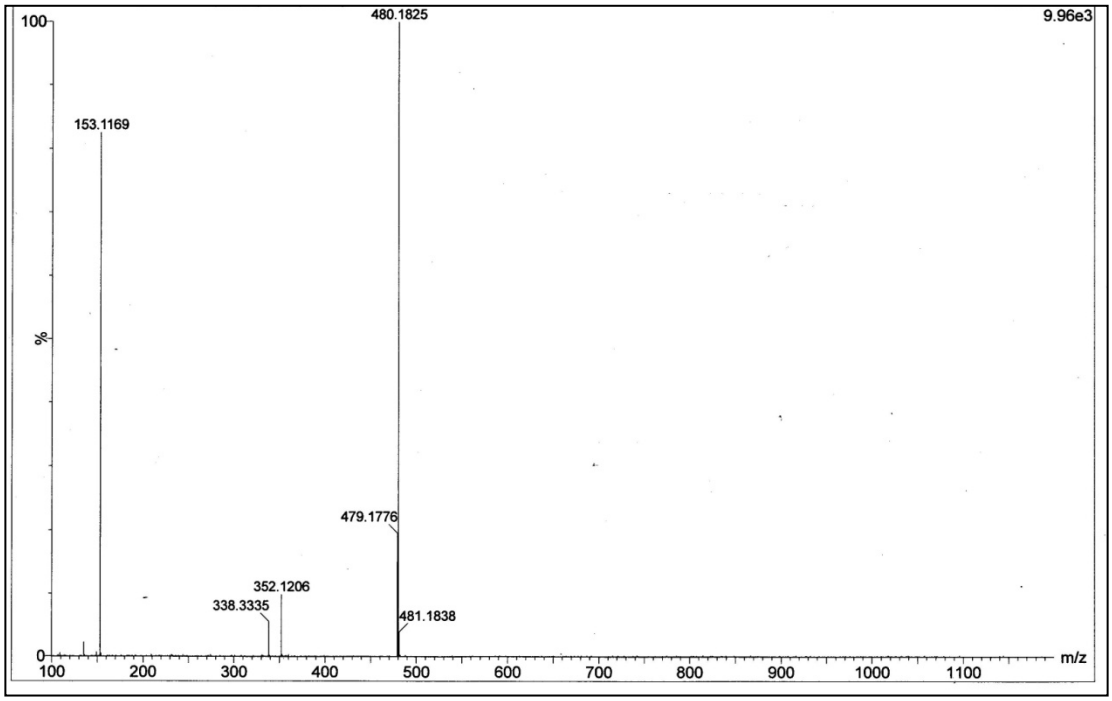

Figure S8: HRMS of the receptor-OCl^- compound.

7. Fluorescence life time spectra of RHQ and RHQ-OCl$^-$ compound:

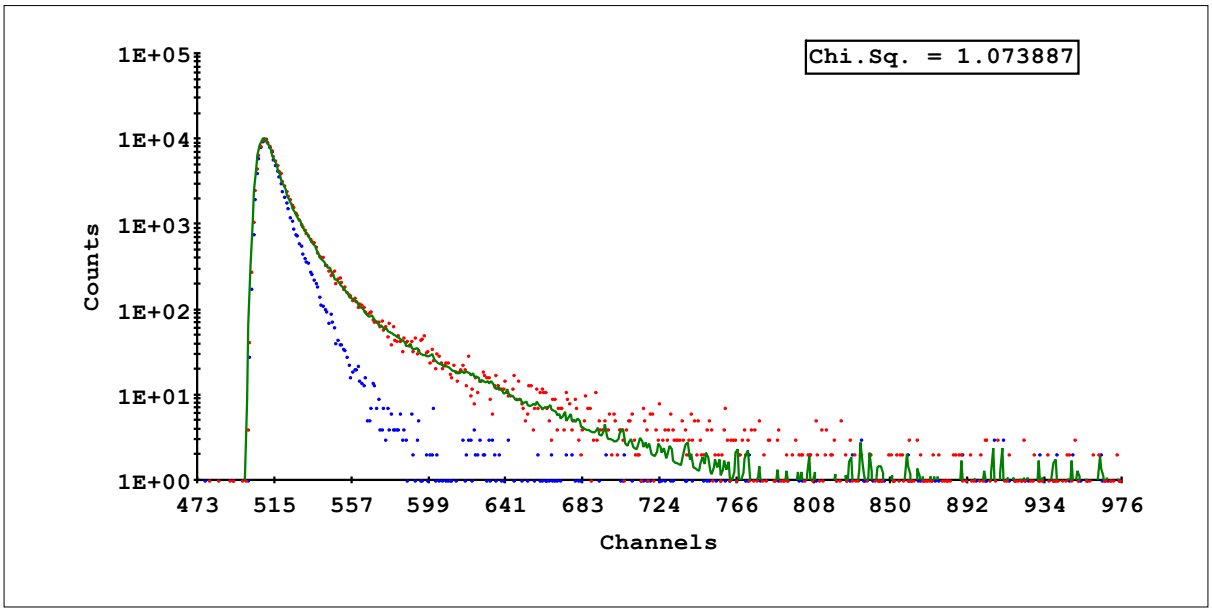

Figure S9: Time-resolved fluorescence decay of RHQ (Red) and prompt (blue)

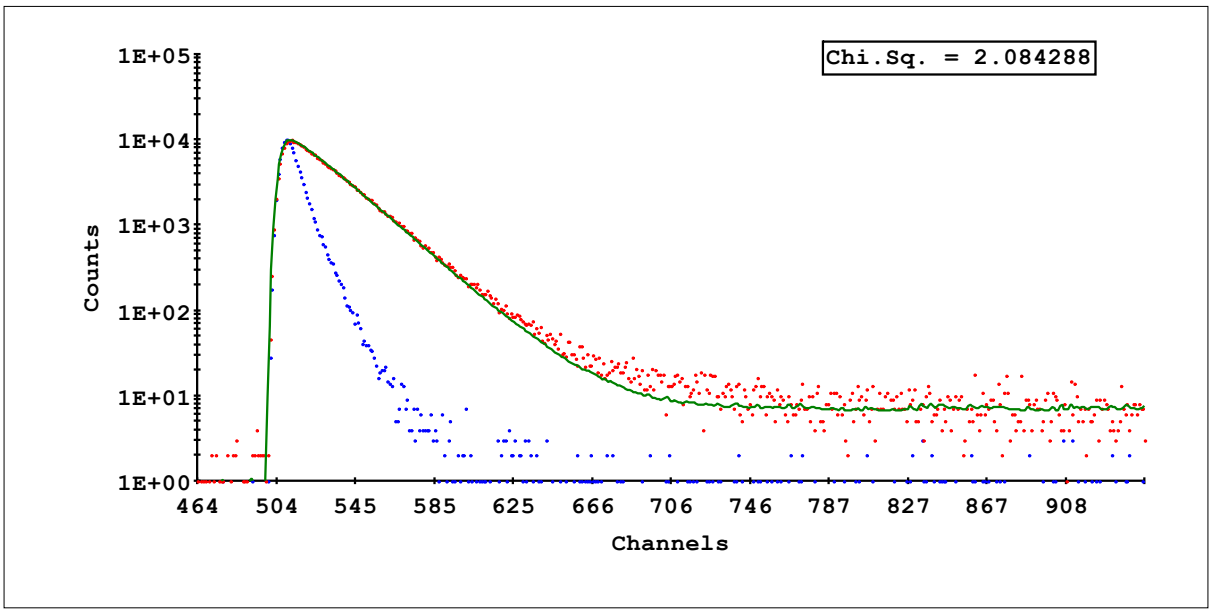

Figure S10: Time-resolved fluorescence decay of RHQ-OCl$^-$ (Red) and prompt (blue)

Table S1: Fluorescence lifetime data

CH_3CN-H_2O (solvent)	Quantum yield *(φ)*	τ (ns)	k_r ($10^8 \times s^{-1}$)	k_{nr} ($10^8 \times s^{-1}$)
RHQ	0.005	0.573	0.08	17.37
RHQ-OCl^-	0.64	2.317	2.76	1.55

8. Computational study:

Method of Calculations

The ground state geometry of RHQ in acetonitrile (CH_3CN) solution has been fully optimized by using the B3LYP functional of DFT method (a hybrid exchange-correlation functional (Becke + Slater + HF exchange and LYP + VWN5 correlations)) [1-3] for the 6-31G** basis set. The stability of the geometry (Figs. 1) on the potential energy surface has been checked by calculating the harmonic vibrational frequencies at the same level which are found to be real. The solvent effect on the ground state geometry of RHQ has been calculated by employing the polarizable continuum model (PCM) [4,5] of solvent at the B3LYP/6-31G** level. In the PCM model the polarized solute-solvent interaction considers geometry relaxation of solute in equilibrium with the solvent reaction field. The solvent-modified transition energy and the oscillator strength corresponding to 40 lowest lying singlet excited states have been calculated by using the PCM solvent model in the framework of time-dependent density functional (TD-DFT) method using the B3LYP functionals for the 6-31G** basis set and the corresponding solvent-modified geometry of the molecule**.** All calculations have been carried out using the GAUSSIAN 09 program suite [6].

Table S2. Experimental and calculated transition wavelength (λ_{max} (**nm**), oscillator strength (**f_0, au)** along with the dominant electronic transitions and corresponding weights obtained for RHQ in the acetonitrile solvent.

λ_{max} (Exp.)	λ_{max} (Theo.)	f_0	**Nature of OPA**	**weight (%)**
308 nm	295.2 nm	0.250	HOMO → LUMO+4	55.7

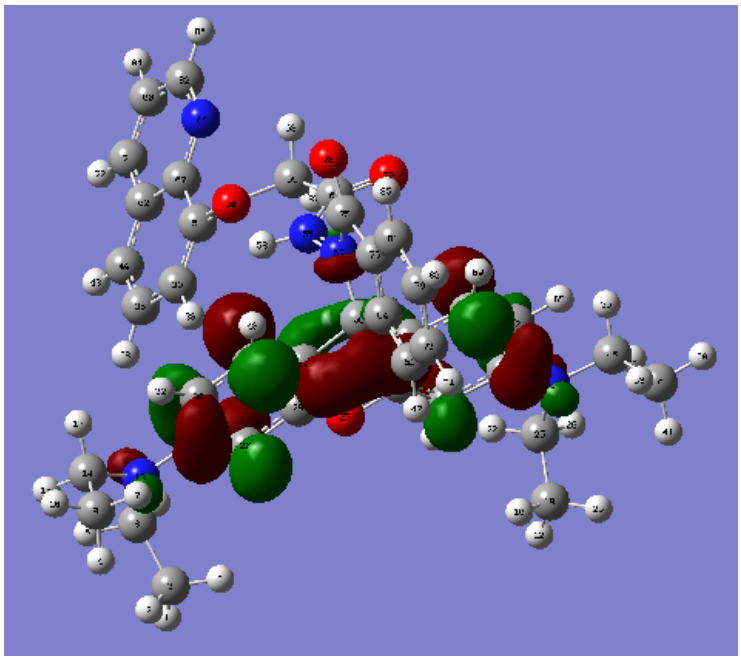

Figure S11. The three dimensional plots of HOMO of RHQ

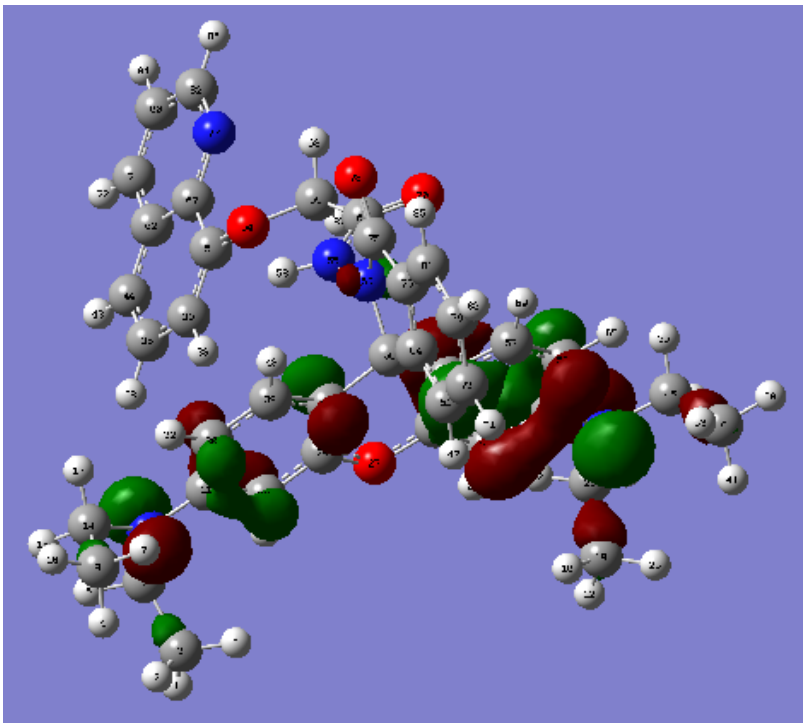

Figure S12. The three dimensional plots of LUMO+4 of RHQ

9. X-ray Crystallography Study:

Single crystal X-ray diffraction data was collected on Bruker APEX Duo CCD area-detector diffractometer operating at 50kV and 30mA using Mo Kα radiation (λ = 0.71073 Å). Diffraction data for RHQ was collected with the Oxford Cryosystem Cobra low temperature attachment at 100.0 (1) K [7]. Data collection and reduction were performed using the APEX2 and SAINT software [8]. The SADABS software was used for absorption correction [8]. The structure was solved by direct method and refinement was carried out by the full-matrix least-squares technique on F^2 using SHELXTL package [9]. All non-hydrogen atoms were refined anisotropically whereas hydrogen atoms were refined isotropically. A summary of the crystallographic data is given in Table 1. All N-bound H atoms were located in difference Fourier maps and fixed at their found positions and refined with $U_{iso}(H) = 1.2\ U_{eq}$ (N). The hydrogen atoms bound to C atoms were positioned geometrically with U_{iso} (H) = 1.2 or 1.5 U_{eq} (C). A rotating-group model was applied for the methyl groups. Three of the terminal ethyl groups attached to N atoms for molecules *A* and *B* are disordered over two sites with refined site occupancies ratio "0.599(11):0.401(11)"/ "0.715(11):0.285(11)"/ "0.688(13):0.312(13)" and "0.670(18): 0.330(18)"/ "0.52(2):0.48(2)"/ "0.801(12):0.199(12)", respectively. Similarity and simulation restraints were applied. The thermal ellipsoids of pair of atoms "N4B C23B" were restrained to be equal. .Crystallographic data for RHQ has been deposited at the Cambridge Crystallographic Data Centre with CCDC No 982181. Copy of the data can be obtained free of charge on application to the CCDC, 12 Union Road, Cambridge CB2 IEZ, UK. Fax: +44-(0)1223-336033 or E-Mail: deposit@ccdc.cam.ac.uk.

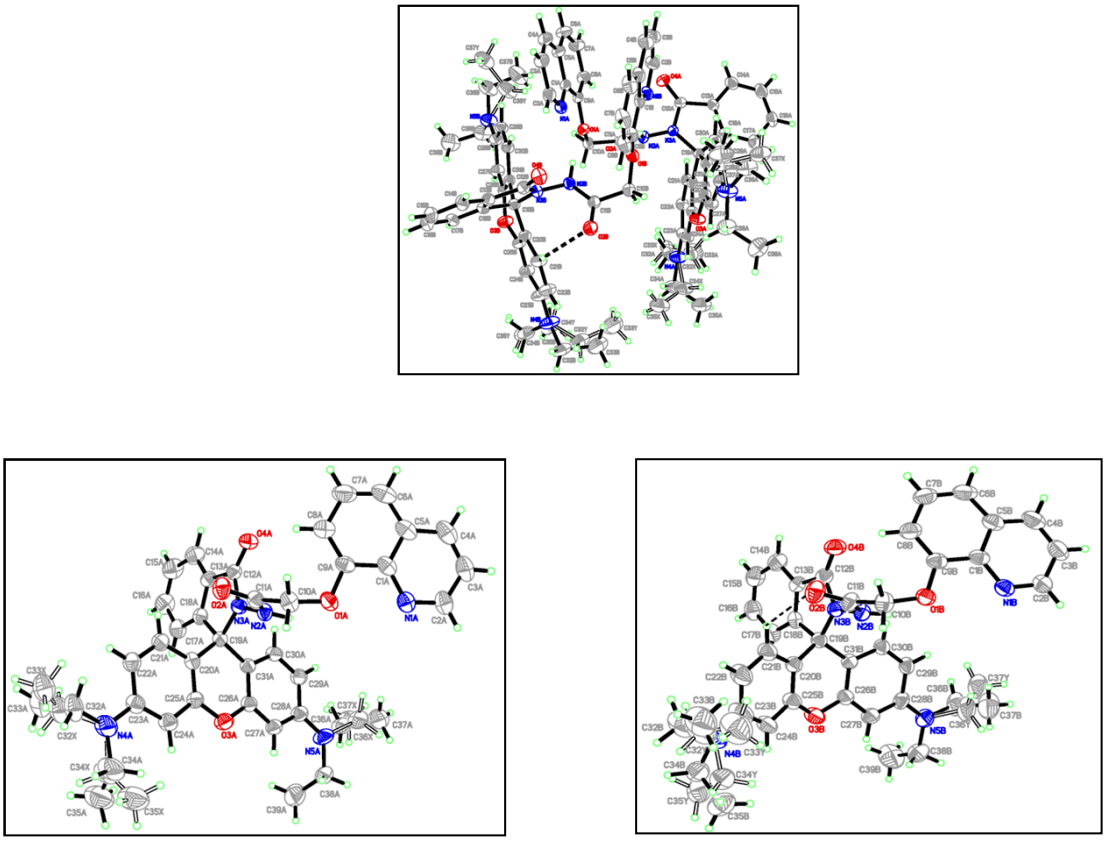

Figure. S13: The molecular structure of (a) asymmetric unit (b) molecule *A* and (c) molecule *B*, of RHQ showing 30% probability displacement ellipsoids for non-H atoms and the atom-numbering scheme. The minor disorder components are indicated with open bonds. Intramolecular hydrogen bonds are drawn as dashed lines.

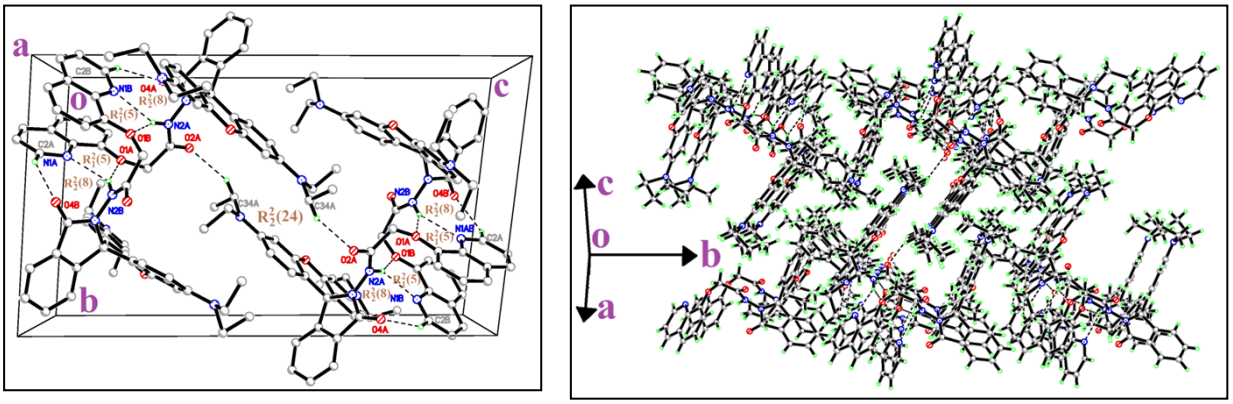

Figure S14: (a) Partial crystal packing of RHQ (within an unit cell), viewed down the a axis, showing $R^2_1(5)$, $R^2_2(8)$ and $R^2_2(24)$ ring motifs. (b) Crystal packing of RHQ showing molecules stacked along c-axis. Hydrogen bonds are drawn as dashed lines. Only major disorder component is shown.

Table S3: X-ray crystallographic data

Compound	RHQ (CCDC 982181)
Formula	$C_{39}H_{39}N_5O_4$
Formula weight	641.75
Crystal system	Triclinic
Space group	*P*-1
T, K	100
Z	4
a,Å	12.0129 (13)
b,Å	13.4609 (14)
c,Å	22.928 (2)
α,deg	94.684 (3)
β,deg	91.243 (3)
γ,deg	102.218 (2)
V, Å^3	3608.6 (7)

d_{calcd} , g/cm^3	1.181
μ, mm^{-1}	0.08
Reflections with $I > 2\sigma(I)$	5644
Independent reflections	12581
θ range, deg	1.6–25.0
hkl range	$h = -14 \rightarrow 14$ $k = -16 \rightarrow 16$ $l = -27 \rightarrow 27$
GOF (F^2)	1.02
R_{int}, R_1, wR_2	0.074, 0.066,0.235
Completeness, %	99.0
T_{min}, T_{max}	0.979, 0.992

Table S4. Hydrogen-bond geometry (Å, º)

D—H···*A*	*D*—H	H···*A*	*D*···*A*	*D*—H···*A*
N2*A*—H1*N*2···O1*B*	0.87	2.33	3.099 (4)	148
N2*A*—H1*N*2···N1*B*	0.87	2.31	3.030 (4)	140
N2*B*—H2*N*2···O1*A*	0.89	2.23	3.048 (4)	151
N2*B*—H2*N*2···N1*A*	0.89	2.39	3.119 (4)	139
C2*A*—H2*AA*···O4*B*	0.93	2.60	3.373 (6)	141
C2*B*—H2*BA*···O4*A*	0.93	2.53	3.342 (5)	146
C21*B*—H21*B*···O2*B*	0.93	2.40	3.033 (5)	125
C34*A*—H34*A*···O2*A*^{i}	0.97	2.50	3.408 (18)	156

Symmetry code: (i) −*x*, −*y*+1, −*z*+1.

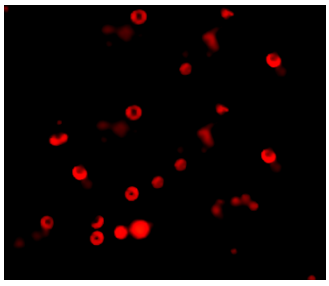

Figure S15: Fluorescence Microscopic photographs of PBMCs (left) without any treatment and (right) treated with RHQ (50 μM)

Reference:

1. A. D. Becke, J. Chem. Phys. 98, 5648 (1993).

2. P. J. Stephens, F. J. Devlin, C. F. Chablowski and M. J. Frisch, J. Phys. Chem. 98, 11623 (1994).

3. R. H. Hertwig and W. Koch, Chem. Phys. Lett. 268, 345 (1997).

4. V. Barone, M. Cossi, J. Phys. Chem. A. 1998, 102, 1995.

5. M. Cossi, N. Rega, G. Scalmani, V. Barone, J. Comp. Chem, 2003, 24, 669.

6. M.J. Frisch, et al. Gaussian 09, Revision B.01, Gaussian, Inc., Wallingford CT, 2010.

7. Cosier, J.; Glazer, A. M. A nitrogen-gas-stream cryostat for general X-ray diffraction studies. J. Appl. Cryst.1986, 19, 105–107.

8. Bruker. APEX2, SAINT and SADABS. Bruker AXS Inc.: Madison, WI, USA, 2009.

9. Sheldrick, G.M. A short history of SHELX. Acta Cryst. 2008, A64, 112-122.